



## Development of novel adenosine receptor ligands based on the 3-amidocoumarin scaffold



Maria J. Matos<sup>a,\*</sup>, Santiago Vilar<sup>b,c</sup>, Sonja Kachler<sup>d</sup>, Maria Celeiro<sup>b</sup>, Saleta Vazquez-Rodriguez<sup>a</sup>, Lourdes Santana<sup>b</sup>, Eugenio Uriarte<sup>b</sup>, George Hripcsak<sup>c</sup>, Fernanda Borges<sup>a,\*</sup>, Karl-Norbert Klotz<sup>d</sup>

<sup>a</sup> CIQUP, Departamento de Química e Bioquímica, Faculdade de Ciências, Universidade do Porto, 4169-007 Porto, Portugal

<sup>b</sup> Departamento de Química Orgánica, Facultad de Farmacia, Universidad de Santiago de Compostela, 15782 Santiago de Compostela, Spain

<sup>c</sup> Department of Biomedical Informatics, Columbia University Medical Center, New York, NY 10032, USA

<sup>d</sup> Institut für Pharmakologie und Toxikologie, Universität Würzburg, 97078 Würzburg, Germany

### ARTICLE INFO

#### Article history:

Received 12 February 2015

Available online 22 May 2015

#### Keywords:

3-Amidocoumarins

Adenosine ligands

Theoretical ADME properties

Molecular modeling calculations

### ABSTRACT

With the aim of finding new adenosine receptor (AR) ligands presenting the 3-amidocoumarin scaffold, a study focusing on the discovery of new chemical entities was carried out. The synthesized compounds **1–8** were evaluated in radioligand binding ( $A_1$ ,  $A_{2A}$  and  $A_3$ ) and adenylyl cyclase activity ( $A_{2B}$ ) assays in order to determine their affinity for human AR subtypes. The 3-benzamide derivative **4** showed the highest affinity of the whole series and was more than 30-fold selective for the  $A_3$  AR ( $K_i = 3.24 \mu\text{M}$ ). The current study supported that small structural changes in this scaffold allowed modulating the affinity resulting in novel promising classes of  $A_1$ ,  $A_{2A}$ , and/or  $A_3$  AR ligands. We also performed docking calculations in  $hA_{2A}$  and  $hA_3$  to identify the hypothetical binding mode for the most active compounds. In addition, some ADME properties were calculated in order to better understand the potential of these compounds as drug candidates.

© 2015 Elsevier Inc. All rights reserved.

### 1. Introduction

Adenosine receptors (ARs) are members of the G-protein-coupled receptor family and represent important pharmacological targets in the treatment of a variety of diseases in which different stressful processes, such as inflammation, hypoxia, ischemia or trauma, are involved [1–3]. Their presence on almost every cell in different organs makes them an interesting target for the pharmacological intervention in many pathophysiological situations [4]. Adenosine plays its many roles through binding to one or more of the four AR subtypes  $A_1$ ,  $A_{2A}$ ,  $A_{2B}$  and  $A_3$  [5]. All the AR subtypes are closely related to specific biochemical processes, therefore they are involved in different pathologies.  $A_1$  ligands are being investigated as promising agents in the therapy of cardiovascular diseases and pain [6].  $A_{2A}$  AR ligands are important compounds for the treatment of neurodegenerative diseases, specifically Alzheimer's and Parkinson's diseases [7].  $A_{2B}$  antagonists and dual  $A_{2B}/A_3$  antagonists are under development due to the role they play in asthma and diabetes and selective adenosine  $A_3$  agonists and antagonists are under consideration for the

treatment of cancer [8]. Finally,  $A_3$  AR ligands have been linked to inflammatory diseases, such as rheumatoid arthritis and psoriasis, liver cancer, neurodegeneration, hepatitis, asthma and to the protective effects in cardiac ischemia and liver regeneration [4]. In the last years, the search for selective and potent ligands toward individual AR subtypes has been intensified, as the role of these AR in many therapeutic areas is continuously expanding [4–6].

Coumarins are an important family of compounds extensively studied and described due to their significant role in medicinal chemistry [9,10]. The simplicity of the chemical framework, the synthetic accessibility and substitution variability of these heterocyclic compounds make them relevant molecules with different properties such as anti-cancer, antiviral, anti-inflammatory, antimicrobial, enzyme-inhibition and antioxidant [11]. Our research group has described different coumarins as potential AR ligands [12–14]. In particular, some amide and carbamate derivatives were studied [14]. The activity profile depicted by some previously described aliphatic amidocoumarins was the basis for this new study [14]. To further explore the importance of this framework as the basis for AR ligands, a selected series of coumarin derivatives bearing an  $\alpha$ - $\beta$  unsaturated bond (aliphatic, aromatic or heteroaromatic) attached to the amide group was synthesized, purified and characterized. Pharmacological evaluation, theoretical

\* Corresponding authors.

E-mail addresses: [mariacmatos@gmail.com](mailto:mariacmatos@gmail.com) (M.J. Matos), [mfernandamborges@gmail.com](mailto:mfernandamborges@gmail.com) (F. Borges).

evaluation of ADME properties, docking calculations and SAR studies of the new series of the amidocoumarins **1–8** were also carried out. To deeply study this family of compounds, and to complete the previous results [14], with the compounds described in this manuscript we also performed docking calculations to better understand the activity and selectivity against the four AR.

## 2. Materials and methods

### 2.1. Chemistry

Starting materials and reagents were obtained from commercial suppliers and were used without further purification (Sigma–Aldrich). Melting points (mp) are uncorrected and were determined with a Reichert Kofler thermopan or in capillary tubes in a Büchi 510 apparatus.  $^1\text{H}$  NMR (300 MHz) and  $^{13}\text{C}$  NMR (75.4 MHz) spectra were recorded with a Bruker AMX spectrometer using  $\text{CDCl}_3$  as solvent. Chemical shifts ( $\delta$ ) are expressed in ppm using TMS as an internal standard. Coupling constants ( $J$ ) are expressed in Hz. Spin multiplicities are given as s (singlet), dd (doublet of doublets), td (triplet of doublets) and m (multiplet). Mass spectrometry was carried out with a Hewlett-Packard-5972-MSD spectrometer. Elemental analyses were performed with a Perkin Elmer 240B microanalyzer and are within 0.4% of calculated values in all cases. Flash chromatography (FC) was performed on silica gel (Merck 60, 230–400 mesh); analytical TLC was performed on pre-coated silica gel plates (Merck 60 F254). Organic solutions were dried over anhydrous  $\text{Na}_2\text{SO}_4$ . Concentration and evaporation of the solvent after reaction or extraction was carried out on a rotary evaporator (Büchi Rotavapor) operating at reduced pressure. The analytical results showed >95% purity for all compounds.

#### 2.1.1. Preparation of the precursor 3-amino-4-hydroxycoumarin

The commercially available 4-hydroxy-3-nitrocoumarin (Sigma–Aldrich) (2.5 mmol) was dissolved in ethanol and a catalytic amount of Pd/C was added to the mixture. The solution was stirred, at room temperature, under  $\text{H}_2$  atmosphere, for 5 h. After the completion of the reaction, the mixture was filtered to eliminate the catalyst. The obtained crude product was then purified by FC (hexane/ethyl acetate, 9:1) to give the desired coumarin, in a yield of 90%.

#### 2.1.2. General procedure for the preparation of 3-amidocoumarins **1–8**

The 3-aminocoumarin (Sigma–Aldrich) or 3-amino-4-hydroxycoumarin (1 mmol) was dissolved in dichloromethane (9 mL), then pyridine (1.1 mmol) was added and the mixture was cooled to  $0^\circ\text{C}$ . Differently substituted acid chloride (Sigma–Aldrich) (1.1 mmol) was added drop-wise at this temperature, and the mixture was stirred overnight at room temperature. The batch was evaporated and purified by column chromatography (hexane/ethyl acetate, 9:1) to give the desired compounds **1–8** [15–18].

### 2.2. Pharmacology

The affinity of compounds **1–8** for the human AR subtypes  $hA_1$ ,  $hA_{2A}$ ,  $hA_3$ , was determined with radioligand competition experiments in Chinese hamster ovary (CHO) cells that were stably transfected with the individual receptor subtypes. The radioligands used were 1 nM (2R,3R,4S,5R)-2-(2-chloro-6-cyclopentylamino-purin-9-yl)-5-hydroxymethyl-tetrahydro-3,4-diol ( $[^3\text{H}]\text{CCPA}$ ) for  $hA_1$ , 10 nM (1-(6-amino-9H-purin-9-yl)-1-deoxy-N-ethyl- $\beta$ -D-ribofuronamide) ( $[^3\text{H}]\text{NECA}$ ) for  $hA_{2A}$ , and 1 nM 2-(1-hexynyl)-N<sup>6</sup>-methyladenosine ( $[^3\text{H}]\text{HEMADO}$ ) for  $hA_3$

receptors. The results were expressed as  $K_i$  values (dissociation constants), which were calculated with the program SCTFIT [19]. Due to the lack of a suitable radioligand for  $hA_{2B}$  receptors, the potency of antagonists at the  $hA_{2B}$  receptor (expressed on CHO cells) was determined by inhibition of NECA-stimulated adenylyl cyclase activity. The 50% inhibitory concentration ( $\text{IC}_{50}$ ) for inhibition of cAMP (cyclic adenosine monophosphate) production was determined and converted to a  $K_i$  value using the Cheng and Prusoff equation.  $K_i$  values (Table 1) are reported as geometric means of three independent experiments with each tested concentration of compound measured in duplicate. As an interval estimate for the dissociation constants, 95% confidence intervals are given in parentheses. Details for pharmacological experiments are described in previous work [13].

### 2.3. Docking calculations

We used the Molecular Operating Environment (MOE) software [20] and the Schrödinger package [21] to carry out homology modeling of the  $hA_3$  AR and molecular docking simulations, respectively.

Glide SP [22] molecular docking simulations were carried out for the most active compounds for the  $hA_{2A}$  and  $hA_3$  receptors to rationalize the selectivity shown by the compounds. To run the calculations we used the  $hA_{2A}$  crystal structure (PDB: 3EML) [23] and a homology model for the  $hA_3$ . The protein pocket structure and the hypothetical binding modes for the compounds were optimized through MM–GBSA in Prime [24]. Using this protocol RMSD values of 0.69 and 1.90 between the calculated and the co-crystallographic poses of the ligands in the 3EML [23] and 3UZC [25]  $hA_{2A}$  receptors were obtained.

#### 2.3.1. Homology modeling

We used the  $hA_{2A}$  crystallized structure (PDB: 3EML) [23] as a template to generate the models. We followed the same protein alignment as described by Katritch et al. [26], considering the most conserved residues in the TM helices. We assessed the protein geometry taking into account Phi–Psi angles and Ramachandran plots, bond lengths, bond angles, dihedrals, side chain rotamers, and non-bonded contacts. We docked high affinity ligands to the  $hA_3$  homology model through the Induce Fit Docking Workflow [21] to optimize the protein pocket. Different protein pocket conformations were evaluated for their ability to discriminate: (1) true

**Table 1**

Binding affinity of coumarins **1–8** for human  $A_1$ ,  $A_{2A}$  and  $A_3$  ARs expressed in CHO cells.

Comp.	$hA_1$	$hA_{2A}$	$hA_3$	Selectivity	
	$K_i$ ( $\mu\text{M}$ )	$K_i$ ( $\mu\text{M}$ )	$K_i$ ( $\mu\text{M}$ )	$hA_1/hA_3$	$hA_{2A}/hA_3$
<b>1</b> [14]	53.9 (35.9–81.1)	>100	7.16 (5.70–9.00)	7.5	>14
<b>2</b>	8.95 (5.60–14.3)	12.2 (8.98–16.7)	>100	<0.09	<0.12
<b>3</b>	>100	>100	>100	–	–
<b>4</b>	>100	>100	3.24 (2.85–3.69)	>31	>31
<b>5</b>	>100	>100	>100	–	–
<b>6</b>	>100	>100	>100	–	–
<b>7</b>	16.2 (8.68–30.2)	>100	>60	<0.27	–
<b>8</b>	5.18 (3.44–7.79)	>100	9.79 (7.66–12.5)	0.53	>10
Theophylline [13]	6.77 (4.07–11.30)	>1.71 (1.02–2.90)	86.40 (73.60–101.30)	0.08	>1.2

Values are geometric means of three experiments and given with 95% confidence intervals in parentheses.

ligands from decoys, and (2) different sets of sub-type selective high affinity compounds. We used ROC curves to assess performance in the tests. The best homology model showed an area under the ROC curve (AUROC) for test 1 of 0.92 (22  $hA_3$  true positive ligands collected in Katritch et al. [26] and 200 random decoys) and for test 2 of 0.82 (22  $hA_3$  true positives and 22  $hA_{2A} + 22 hA_1$  compounds as false positives) [26]. The best  $hA_3$  models were retained for further docking studies.

#### 2.4. Theoretical evaluation of absorption, distribution, metabolism and excretion properties

The absorption, distribution, metabolism and excretion (ADME) properties of the studied compounds were calculated using the Molinspiration property programme. LogP was calculated using the methodology developed by Molinspiration [27] as a sum of fragment-based contributions and correction factors. Topological polar surface area (TPSA) was calculated based on the methodology published by Ertl et al. as a sum of fragment contributions [28]. Oxygen and nitrogen-centered polar fragments were considered. Polar surface area (PSA) has been shown to be a very good descriptor characterizing drug absorption, including intestinal absorption, bioavailability, Caco-2 permeability and blood–brain barrier penetration. The method for calculation of molecule volume developed at Molinspiration is based on group contributions. These have been obtained by fitting the sum of fragment contributions to ‘real’ three-dimensional (3D) volume for a training set of about 12,000, mostly drug-like molecules. 3D molecular geometries for a training set were fully optimized by the semi-empirical AM1 method.

### 3. Results and discussion

#### 3.1. Chemistry

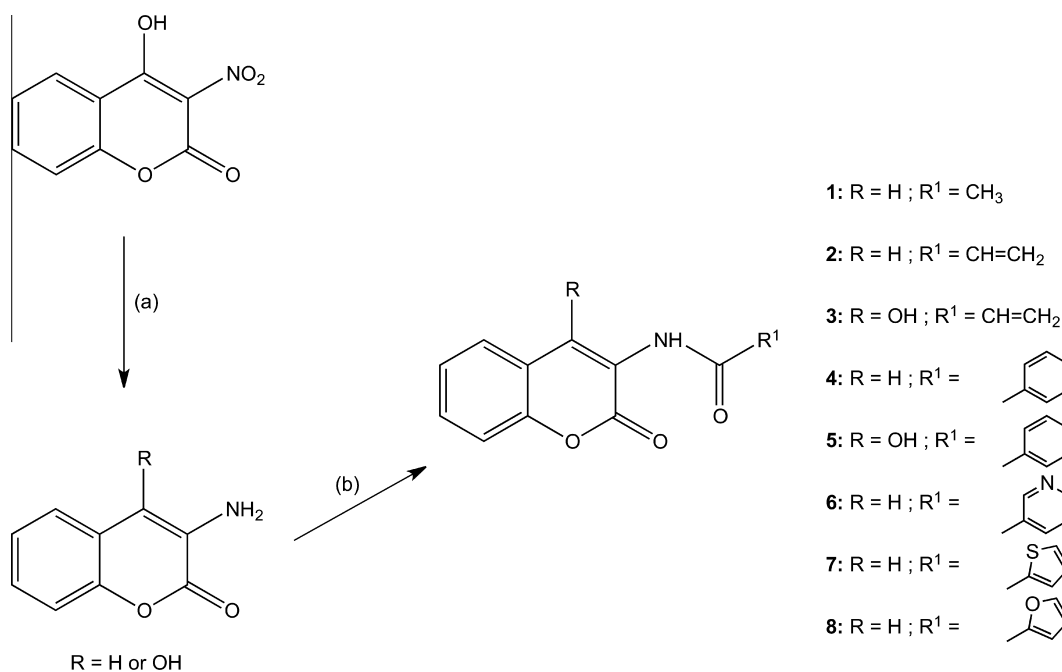
The described derivatives were efficiently synthesized according to the protocol outlined in Scheme 1. Coumarins **1–8** were prepared starting from 3-aminocoumarin or from 3-amino-4-hydroxycoumarin, which were synthesized as previously described [13,15]. The 3-amino-4-hydroxycoumarin was

prepared by a reduction of the commercially available 3-nitro-4-hydroxycoumarin, in ethanol, with Pd/C as catalyst, in  $H_2$  atmosphere, with a yield of 90% [13]. An acylation reaction of the 3-aminocoumarins with the conveniently substituted acid chloride, using pyridine in dichloromethane, from 0 °C to room temperature, afforded the differently substituted 3-amidocoumarins (**1–8**) in yields between 80% and 90% [14–18]. The reaction conditions and chemical characterization of the new compounds are detailed in methods.

**N-(Coumarin-3-yl)acrylamide (2)** Yield: 84%. mp: 168–169 °C.  $^1H$  NMR (300 MHz,  $CDCl_3$ ): 5.90 (dd, 1H, CH,  $J = 9.9, J = 1.5$  Hz), 6.35 (dd, 1H,  $CH_2$ ,  $J = 16.9, J = 9.9$  Hz), 6.51 (dd, 1H,  $CH_2$ ,  $J = 16.9, J = 1.5$  Hz), 7.30–7.38 (m, 2H, H-6, H-8), 7.46–7.57 (m, 2H, H-5, H-7), 8.28 (s, 1H, NH), 8.82 (s, 1H, H-4).  $^{13}C$  NMR (75 MHz, DMSO- $d_6$ )  $\delta$  (ppm): 111.6, 115.1, 119.1, 119.2, 120.5, 123.2, 124.3, 125.1, 125.7, 145.3, 154.1, 159.6. MS  $m/z$  (%): 216 (12), 215 ( $M^+$ , 80), 161 (97), 133 (27), 104 (11), 77 (22), 55 (100). Anal. Elem. Calc. for  $C_{12}H_9NO_3$ : C, 66.97; H, 4.22. Found: C, 66.98; H, 4.25.

**N-(4-Hydroxycoumarin-3-yl)acrylamide (3)** Yield: 80%. mp: 159–160 °C.  $^1H$  NMR (300 MHz,  $CDCl_3$ ): 6.01 (dd, 1H, CH,  $J = 9.9, J = 1.3$  Hz), 6.45 (dd, 1H,  $CH_2$ ,  $J = 16.7, J = 9.9$  Hz), 6.60 (dd, 1H,  $CH_2$ ,  $J = 16.7, J = 1.3$  Hz), 7.36–7.43 (m, 2H, H-6, H-8), 7.58 (td, 1H, H-7,  $J = 7.5, J = 1.6$  Hz), 8.04 (dd, 1H, H-5,  $J = 7.9, J = 1.6$  Hz), 8.31 (s, 1H, NH), 13.95 (s, 1H, OH).  $^{13}C$  NMR (75 MHz, DMSO- $d_6$ ): 102.5, 115.5, 117.0, 119.8, 124.9, 125.1, 126.1, 130.4, 151.3, 160.0, 164.3, 167.5. MS  $m/z$  (%): 232 (9), 231 ( $M^+$ , 44), 177 (71), 148 (11), 121 (40), 65 (16). Anal. Elem. Calc. for  $C_{12}H_9NO_4$ : C, 62.34; H, 3.92. Found: C, 62.36; H, 3.95.

**N-(Coumarin-3-yl)furan-2-carboxamide (8)** Yield: 90%. mp: 183–184 °C.  $^1H$  NMR (300 MHz, DMSO- $d_6$ ): 6.74 (dd, 1H, H-4',  $J = 3.6, J = 1.8$  Hz), 7.34–7.58 (m, 4H, H-5, H-6, H-8, H-5'), 7.77 (td, 1H, H-7,  $J = 8.0, J = 1.4$  Hz), 8.00 (dd, 1H, H-3',  $J = 1.8, J = 0.8$  Hz), 8.58 (s, 1H, H-4), 9.26 (s, 1H, NH).  $^{13}C$  NMR (75 MHz, DMSO- $d_6$ ): 112.1, 113.2, 115.7, 116.8, 122.9, 124.3, 126.2, 126.8, 127.7, 145.8, 146.5, 149.5, 155.3, 159.8. MS  $m/z$  (%): 256 (16), 255 ( $M^+$ , 79), 227 (7), 132 (6), 95 (100), 77 (10). Anal. Elem. Calc. for  $C_{14}H_9NO_4$ : C, 65.88; H, 3.55. Found: C, 65.86; H, 3.53.



**Scheme 1.** Reagents and conditions: (a)  $H_2$ , EtOH, Pd/C, r.t., 5 h; (b)  $R_1COCl$ , pyridine, dichloromethane, 0 °C to r.t., overnight.

### 3.2. Pharmacological study

The affinity of the synthesized 3-amidocoumarins for A<sub>1</sub>, A<sub>2A</sub>, and A<sub>3</sub> ARs was tested in radioligand binding assays. The affinity for the A<sub>2B</sub> AR was determined in a functional assay (inhibition of agonist-stimulated adenylyl cyclase activity) [29,30]. The detailed methodology is described in methods. The binding data for A<sub>1</sub>, A<sub>2A</sub> and A<sub>3</sub> ARs are shown in Table 1. None of the derivatives showed measurable affinity for the A<sub>2B</sub> AR ( $K_i > 20 \mu\text{M}$ ).

### 3.3. Theoretical ADME properties

The prediction of the ADME properties plays an important role in the drug design process because these properties account for the failure of about 60% of all drugs in the clinical phases. Therefore, preliminary data for theoretical ADME profiles of the newly synthesized 3-amidocoumarins, were determined (Table 2). The lipophilicity, expressed as the octanol/water partition coefficient (represented as  $\log P$ ), was also calculated using the Molinspiration property calculation program [27,28,31].

From the data obtained, one can notice that all the coumarin derivatives possess  $\log P$  values compatible with those required to cross membranes. From the data obtained from the prediction of ADME properties it can be observed that no violations of Lipinski's rule (molecular weight,  $\log P$ , number of hydrogen donors and acceptors) were found making the coumarin derivatives promising agents. Topological polar surface area (TPSA), described to be a predictive indicator of membrane penetration, is also found to be positive for these potential drugs.

### 3.4. Docking calculations

Since *hA<sub>2A</sub>* and *hA<sub>3</sub>* AR seems to be involved in neurodegenerative pathologies and neuroprotective processes [4,7], in which our group is interested, docking calculations were performed in order to understand structural features related to the activity against these receptors. Compound 2 (bearing an aliphatic amide) as the only derivative with affinity for the *hA<sub>2A</sub>* receptor bound with the coumarin ring orientated toward the bottom of the A<sub>2A</sub> receptor cavity and the acrylamide chain pointing toward the upper region close to the extracellular loops. The carbonyl oxygen in the coumarin ring establishes a hydrogen bond interaction with the amide moiety of the residue Asn253 (Fig. 1a). This hypothetical binding mode agrees with previous results showing the importance of the residue Asn<sup>6.55</sup> (Ballesteros–Weinstein numbering) in ligand recognition [23,32,33]. However, compound 2 does not establish strong interaction in the *hA<sub>3</sub>* with the corresponding residue Asn250. Molecular docking showed a hypothetical binding mode placed in the extracellular area and establishing a possible hydrogen bond with the residue Gln167. This hypothetical binding mode

**Table 2**  
Structural properties of the coumarin derivatives 1–8.<sup>a</sup>

Comp.	$\log P$	Molecular weight (g/mol)	TPSA (Å <sup>2</sup> )	<i>n</i> -OH acceptors	<i>n</i> -OHNH donors	Volume (Å <sup>3</sup> )
1	1.16	203.20	59.31	4	1	176.53
2	1.76	215.21	59.31	4	1	187.70
3	1.47	231.21	79.54	5	2	195.72
4	2.83	265.27	59.31	4	1	231.38
5	2.54	281.27	79.54	5	2	239.40
6	1.60	266.26	72.21	5	1	227.22
7	2.73	271.30	59.31	4	1	222.09
8	2.09	255.23	72.45	5	1	212.95

<sup>a</sup> TPSA, topological polar surface area; *n*-OH, number of hydrogen bond acceptors; *n*-OHNH, number of hydrogen bond donors. The data was determined with Molinspiration calculation software [27].

in the *hA<sub>3</sub>* showed an energy contribution in the interaction with different residues distinct from the mode of interaction with the *hA<sub>2A</sub>* AR (Fig. 1b). This result is in accordance with the lack of affinity of compound 2 for the *hA<sub>3</sub>* AR. The interaction scores are calculated as the sum of Coulomb, *van der Waals* and hydrogen bonding energies. Fig. 1b also shows the importance of the residue Phe168 in ligand recognition.

Compound 4, the most potent A<sub>3</sub> AR ligand in the series, showed a hypothetical binding mode similar to compound 2. The compound docked to the *hA<sub>3</sub>* AR orientated the benzamide substituent toward the upper region of the cavity and the coumarin ring is located in the bottom of the pocket (Fig. 2a). The phenyl group of the compound is located close to the hydrophobic residues Val169 and Leu264 (residues not present in the *hA<sub>2A</sub>*). Lipophilicity and steric size of the substituent seem to be important factors for *hA<sub>3</sub>*AR affinity. Compound 4 also establishes hydrogen bond interactions with the residue Asn250. Previous results performed with other scaffolds at the *hA<sub>3</sub>* AR [32,33] showed similar ligand poses as reported in this study. Although a similar binding mode was found for compound 4 in the *hA<sub>2A</sub>* AR, the compound is placed slightly shifted toward the upper region causing a disruption in the interaction energy with the residue Asn250 (Fig. 2b and c). Other possible binding modes of compound 4 extracted from docking studies for the *hA<sub>2A</sub>* did not show relevant interactions with the cited residue. Additional information on the selectivity between *hA<sub>2A</sub>* and *hA<sub>3</sub>* was also acquired by calculating the residue energy contributions to the interaction with compound 4 (Fig. 2c).

### 3.5. Discussion

A novel series of coumarin derivatives presenting on their structure a common planar N=C=O framework, represented by an

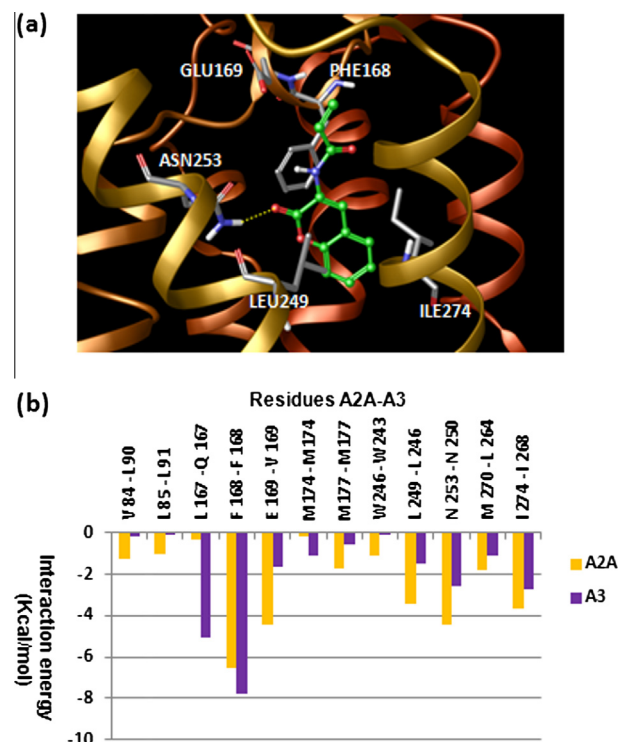


**Fig. 1.** (a) Hypothetical binding mode for compound 2 (green carbons) calculated through docking to the *hA<sub>2A</sub>* AR. Important residues in the protein–ligand interaction are shown in tube (gray carbons). Hydrogen bond interaction between compound 2 and residue Asn253 is colored in yellow. (b) Residue interaction scores (sum of Coulomb, *van der Waals* and hydrogen bonding interactions) for compound 2 in the *hA<sub>2A</sub>* and the *hA<sub>3</sub>* AR.

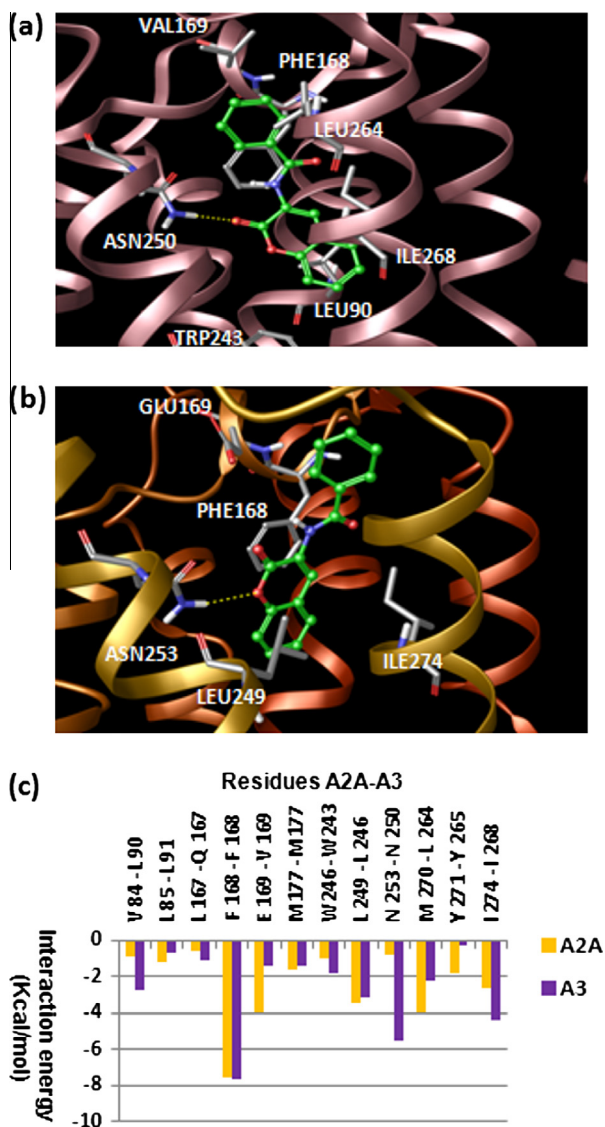


**Fig. 2.** (a) Binding pose calculated through molecular docking for compound **4** (green carbons) in the *hA<sub>3</sub>*. Important residues in the interaction between the ligand and the protein are shown in tube (gray carbons). Hydrogen bonds are represented in yellow. (b) Hypothetical binding mode for compound **4** (green carbons) in the *hA<sub>2A</sub>*. (c) Residue contributions in the ligand–protein interaction (sum of Coulomb, *van der Waals* and hydrogen bonding interactions) for compound **4** in the *hA<sub>2A</sub>* and the *hA<sub>3</sub>* AR.

amidic group at position 3, were studied for their ability to bind the four ARs. Different alkyl, aromatic or heteroaromatic groups were attached to the amidic function at position 3 and the effect of these substitutions on affinity was studied. In addition, the presence or the absence of a hydroxyl group at position 4 was also explored. As according to a previous study [14], none of the 4-hydroxy derivatives (compounds **3** and **5**) displayed binding affinity for any AR subtype. The presence of a hydroxyl function at position 4 of the coumarin skeleton is not tolerated, notwithstanding the presence of an aliphatic (compound **3**), or an aromatic (compound **5**) group at position 3.

The structurally simpler derivative of the series (compound **1**) showed affinity for *hA<sub>1</sub>* and *hA<sub>3</sub>* ARs ( $K_i = 53.9 \mu\text{M}$  and  $K_i = 7.16 \mu\text{M}$ , respectively). The introduction of a double bond on

this structure (compound **2**) improved the *A<sub>1</sub>* ( $K_i = 8.95 \mu\text{M}$ ) and *A<sub>2A</sub>* ( $K_i = 12.2 \mu\text{M}$ ) affinity, with a concomitant loss of affinity for the *hA<sub>3</sub>* AR. Compound **2** was the only derivative of the series with affinity for the *hA<sub>2A</sub>* AR. The introduction of an acryl group on the amidic scaffold could help on the design of *hA<sub>2A</sub>* AR ligands.

Comparing compound **1** with the corresponding benzamide derivative **4** reveals a high increase on the *A<sub>3</sub>* affinity of compound **4** ( $K_i = 3.24 \mu\text{M}$ ). In addition, a lack of measurable *A<sub>1</sub>* affinity made compound **4** the most *A<sub>3</sub>* selective compound of this series. The replacement of the benzene ring by a pyridine substituent (compound **6**) led to loss of affinity for all ARs. On the other hand, the substitution by a thiophene ring at the same position (compound **7**) resulted in a selective *hA<sub>1</sub>* AR ligand ( $K_i = 16.2 \mu\text{M}$ ). Finally, the introduction of a furyl ring in place of the thiophene (compound **8**) improved the *hA<sub>1</sub>* AR affinity ( $K_i = 5.18 \mu\text{M}$ ) with a concurrent appearance of a similar *A<sub>3</sub>* affinity ( $K_i \text{ AR} = 9.79 \mu\text{M}$ ). It is interesting to note that the affinity for *hA<sub>1</sub>* and *hA<sub>3</sub>* ARs can be modulated by the choice of heteroatom in the aromatic ring in this position. The results found for compounds **4**, **7** and **8** suggest that 3-amidocoumarin is a promising scaffold to develop ligands with improved *A<sub>1</sub>*, *A<sub>3</sub>*, or dual *A<sub>1</sub>/A<sub>3</sub>* affinity and selectivity. Finally, the results found for compounds **2**, suggest that 3-amidocoumarin is also a promising scaffold to develop *A<sub>2A</sub>* ligands.

All adenosine receptor agonists known to date are adenosine derivatives with the notable exception of a series of 2-aminodicyanopyridine derivatives [6]. We confirmed the antagonistic nature of compound **7** at the *A<sub>1</sub>* adenosine receptor in a GTP-shift experiment (data not shown).

Compounds **1**, **4** and **8** present better *hA<sub>3</sub>* affinity than theophylline, used as reference compound. In addition, compound **4** is *hA<sub>3</sub>* selective ligand, being 27 times more active against *hA<sub>3</sub>* than the reference compound. Regarding *hA<sub>1</sub>* affinity, compounds **2** and **8** present similar  $K_i$  to theophylline.

Our research group has previously described different coumarins as potential AR ligands [12–14]. In particular, the activity profile depicted by some previously described amidocoumarins was the basis for this new study [14]. However, compound **4** of this new series presented with two fold higher affinity for *hA<sub>3</sub>* AR compared to the best compound of the previous study.

To deeply study the new family of compounds, docking calculations were now performed to better understand the activity and selectivity against the four AR. Docking results showed a different hypothetical binding mode for compound **2** into the *hA<sub>2A</sub>* and the *hA<sub>3</sub>* AR. Different energy contributions of individual residues seem to be responsible for the observed AR selectivity. Moreover, in the case of compound **4**, the pose determined through docking presented a lower energy interaction in the *hA<sub>2A</sub>* with the residue Asn253. The calculations showed a reduction in the electrostatic energy contribution possibly due to the repulsion between the carbonyl oxygen of the derivative **4** and the oxygen of the amide in the residue Asn253. As described previously, this residue plays an important role in the interaction with different ligands [23,32,33]. The disruption of this interaction provides a valid explanation for the reduction of *hA<sub>2A</sub>* activity.

Moreover, different residues located in the extracellular area of the ligand binding domain could be very important for ligand entry and stabilization of binding [33], thereby constituting essential attributes for AR selectivity. *hA<sub>3</sub>* bears respective hydrophobic residues, such as Val169 and Leu264 that can favor interactions with hydrophobic substituents like the phenyl group in compound **4**. The corresponding residues in *hA<sub>1</sub>*, the Glu172 and Thr270, showed hydrophilic characteristics more suitable for interaction with polar substituents in the ring. On the other hand, some residues in the

$hA_{2A}$ , such as Glu169 with a negative charge and hydrophilic characteristics or the positively charged His264, are not present in the  $hA_3$ .

#### 4. Conclusion

The 3-amidocoumarin scaffold proved to have potential for the design of novel AR ligands with distinct selectivity profiles for ARs. A detailed analysis of the results obtained so far allowed to conclude that the affinity and/or selectivity of the coumarins toward ARs can be modulated by the nature of the substituents attached to the amidic linker at position 3 of the scaffold. Compound **4** (phenyl derivative) proved to be the best compound of the series, being considered as a starting point for the design and synthesis of new coumarins as  $hA_3$  AR selective ligands. The profile of compound **8** (furyl derivative) suggests this derivative as a lead for ligands with dual  $hA_1/hA_3$  AR selectivity. Compound **7** (thiophenyl derivative) proved to be the only selective  $hA_1$  compound of the studied series, being the inspiration for the design of  $A_1$  selective ligands. The simplicity of the synthetic processes and the decoration capability of the 3-amidocoumarins make them a privileged structure for the development of novel AR ligands. The theoretical evaluation of ADME properties confirms the role of these compounds as promising hits. Additionally, molecular docking simulations have been supportive to explain the selectivity of the most potent ligands for  $hA_{2A}$  and  $hA_3$  ARs.

#### Acknowledgments

This work was partially supported by University of Santiago de Compostela and Spanish researchers personal's funds. MJM gratefully acknowledges Fundação para a Ciência e Tecnologia, POPH (Programa Operacional Potencial Humano) and QREN (Quadro de Referência Estratégica Nacional) for her postdoctoral Grant (SFRH/BPD/95345/2013). SV-R gratefully acknowledges the Universidade do Porto for her postdoctoral fellowship associated to the QREN FCUP-CIQ-UP-NORTE-07-0124-FEDER-000065 project. SV thanks Plan Galego de Investigación, Innovación e Crecemento 2011–2015 (I2C), European Social Fund (ESF) and Angeles Alvariño Program from Xunta de Galicia (Spain).

#### Appendix A. Supplementary material

Supplementary data associated with this article can be found, in the online version, at <http://dx.doi.org/10.1016/j.bioorg.2015.05.008>.

#### References

- [1] C. St Hilaire, S. Carroll, H. Chen, K. Ravid, J. Cell. Physiol. 218 (2009) 35–44.
- [2] P. Baraldi, M. Tabrizi, S. Gessi, P. Borea, Chem. Rev. 108 (2008) 238–263.
- [3] G. Hasko, J. Linden, B. Cronstein, P. Pacher, Nat. Rev. Drug Discov. 7 (2008) 759–770.
- [4] B. Koscsó, B. Csóka, P. Pacher, G. Haskó, Expert Opin. Investig. Drugs 20 (2011) 757–768.
- [5] N. Press, J. Fozard, Expert Opin. Ther. Pat. 20 (2010) 987–1005.
- [6] B. Fredholm, A. Ijzerman, K. Jacobson, J. Linden, C. Müller, Pharmacol. Rev. 63 (2011) 1–34.
- [7] F. Areias, M. Costa, M. Castro, J. Brea, E. Gregori-Puigjané, M.F. Proença, J. Mestres, M.I. Loza, Eur. J. Med. Chem. 54 (2012) 303–310.
- [8] C.E. Müller, K.A. Jacobson, Biochim. Biophys. Acta 1808 (2011) 1290–1308.
- [9] F. Borges, F. Roleira, N. Milhazes, E. Uriarte, L. Santana, Front. Med. Chem. 4 (2009) 23–85.
- [10] M.J. Matos, D. Viña, S. Vazquez-Rodriguez, E. Uriarte, L. Santana, Curr. Top. Med. Chem. 12 (2012) 2210–2239.
- [11] F. Borges, F. Roleira, N. Milhazes, L. Santana, E. Uriarte, Curr. Med. Chem. 12 (2005) 887–916.
- [12] S. Vazquez-Rodriguez, M.J. Matos, L. Santana, E. Uriarte, F. Borges, S. Kachler, K.-N. Klotz, J. Pharm. Pharmacol. 65 (2013) 697–703.
- [13] M.J. Matos, V. Hogger, A. Gaspar, S. Kachler, F. Borges, E. Uriarte, L. Santana, K.-N. Klotz, J. Pharm. Pharmacol. 65 (2013) 1590–1597.
- [14] M.J. Matos, A. Gaspar, S. Kachler, K.-N. Klotz, F. Borges, L. Santana, E. Uriarte, J. Pharm. Pharmacol. 65 (2013) 30–34.
- [15] C.S. Barnes, M.I. Strong, J.L. Ocolowitz, Tetrahedron 19 (1963) 839–847.
- [16] E. Klusmann, W. Rosenthal, J. Rademann, F. Christian, PCT Int. Appl. (2006) (WO2006122546 A120061123).
- [17] V. Maddi, S.N. Mamledesai, D. Satyanarayana, S. Swamy, Ind. J. Pharmacol. Sci. 69 (2007) 847–849.
- [18] L.D.S. Yadav, S. Singh, V.K. Rai, Tetrahedron Lett. 50 (19) (2009) 2208–2212.
- [19] A. De Lean, A.A. Hancock, R. Lefkowitz, J. Mol. Pharmacol. 21 (1982) 5–16.
- [20] MOE, version 2011.10, Chemical Computing Group Inc., <[www.chemcomp.com](http://www.chemcomp.com)>.
- [21] Schrödinger Suite, Schrödinger, LLC, New York, NY, USA, 2011.
- [22] Glide, version 5.7, Schrödinger, LLC, New York, NY, 2011.
- [23] V.P. Jaakola, M.T. Griffith, M.A. Hanson, V. Cherezov, E.Y. Chien, J.R. Lane, A.P. Ijzerman, R.C. Stevens, Science 322 (2008) 1211–1217.
- [24] Prime, version 3.0, Schrödinger, LLC, New York, NY, 2011.
- [25] M. Congreve, S.P. Andrews, A.S. Doré, K. Hollenstein, E. Hurrell, C.J. Langmead, J.S. Mason, I.W. Ng, B. Tehan, A. Zhukov, M. Weir, F.H. Marshall, J. Med. Chem. 55 (2012) 1898–1903.
- [26] V. Katritch, I. Kufareva, R. Abagyan, Neuropharmacology 60 (2011) 108–115.
- [27] M. cheminformatics, Bratislava, Slovak Republic, <<http://www.molinspiration.com/services/properties.html>>.
- [28] P. Ertl, B. Rohde, P. Selzer, J. Med. Chem. 43 (2000) 3714–3717.
- [29] K.-N. Klotz, J. Hessling, J. Hegler, C. Owman, B. Kull, B.B. Fredholm, M.J. Lohse, Naunyn Schmiedebergs Arch. Pharmacol. 357 (1997) 1–9.
- [30] K.-N. Klotz, N. Falgner, S. Kachler, C. Lambertucci, S. Vittori, R. Volpini, G. Cristalli, Eur. J. Pharmacol. 556 (2007) 14–18.
- [31] C.A. Lipinski, F. Lombardo, B.W. Dominy, P.J. Feeney, Adv. Drug Deliv. Rev. 23 (1997) 3–26.
- [32] A. Gaspar, J. Reis, S. Kachler, S. Paoletta, E. Uriarte, K.-N. Klotz, S. Moro, F. Borges, Biochem. Pharmacol. 84 (2012) 21–29.
- [33] O. Lenzi, V. Colotta, D. Catarzi, F. Varano, D. Poli, G. Filacchioni, K. Varani, F. Vincenzi, P.A. Borea, S. Paoletta, E. Morizzo, S. Moro, J. Med. Chem. 52 (2009) 7640–7652.